Sustainable Energy Technologies and Assessments 87 (2026) 104919

Contents lists available at ScienceDirect

Sustainable Energy Technologies and Assessments

journal homepage: www.elsevier.com/locate/seta

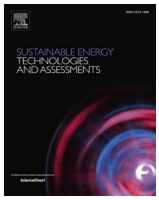

Comparative energy assessment of three glazed courtyard roof designs in a cold climate heritage building

Alejandro Cabeza-Prieto [a,1,*], M. Paz Sáez-Pérez [b,2], M. Soledad Camino-Olea [a,3]

[a] Department of Architectural Constructions, Escuela Técnica Superior de Arquitectura de Valladolid, University of Valladolid, Av. de Salamanca 18, 47014 Valladolid, Spain
[b] Department of Architectural Constructions, Advanced Technical School of Building Engineering, University of Granada, c/ Severo Ochoa s/n, 18071 Granada, Spain

ARTICLE INFO

Keywords:
Courtyard roofing
Bioclimatic architecture
Adaptive reuse
Climate change adaptation
Historic buildings
Passive design strategies

ABSTRACT

The use of translucent roofs over courtyards in historic buildings has become a common strategy in rehabilitation projects. However, many of these interventions are carried out without bioclimatic or energy-efficiency criteria, leading to risks of overheating and thermal discomfort, particularly during summer. This issue is expected to worsen with climate change, compromising the habitability of these spaces.

This study compares the thermal and energy performance of three glazed roof configurations: a triangulated dome, a flat roof, and a south-facing sawtooth roof with vertical glazing. The case study is a Renaissance courtyard located in Burgos, Spain (continental Mediterranean climate). Dynamic simulations using EnergyPlus and Ecotect evaluate solar exposure, annual heating and cooling demand, free-running thermal behavior, and daylight availability.

Results show that roof geometry has a decisive impact on energy efficiency. The sawtooth solution eliminates cooling demand under passive operation and maintains thermal comfort (20–25 °C) throughout the year while ensuring daylight levels above 4000 lx.

These findings support the use of passive geometric strategies to improve climate adaptation in enclosed heritage courtyards. The methodology is replicable in similar cold-climate contexts and offers practical guidance for energy-efficient retrofitting of historic buildings.

Introducción

Throughout history, the courtyard has played a key role in architecture, not only for its spatial functionality but especially of its capacity to regulate microclimates. The bioclimatic performance of courtyards depends fundamentally on their morphology and the surrounding climatic context [1], while recent research emphasizes that geometry also constitutes a direct determinant of energy performance [2,3].

Morphologically, courtyards are open spaces bounded by buildings, with square and rectangular configurations predominating in hot-humid climates [4]. The height-to-width ratio significantly influences thermal comfort [5,6], while aspect ratio, orientation, and albedo condition the microclimate in Mediterranean and Caribbean environments [7,8]. Polygonal, U-shaped, and circular geometries with specific passive potential have also been documented [9,10]. Their persistence across Africa, Asia, Europe, and Latin America demonstrates their climatic and cultural adaptability and confirms the close relationship between geometry and thermal behavior in warm climates [11,12].

Geometry also acts as a passive cooling strategy by enhancing natural ventilation and reducing indoor temperature [13]. Numerical models have confirmed the influence of orientation and degree of enclosure in semi-enclosed courtyards [14]. Its impact is particularly relevant in hot and dry climates [15], where courtyards with high aspect ratios (RA $>$ 3) and low sky view factors (SVF $<$ 0.1) exhibit greater diurnal and nocturnal thermal attenuation. Studies have reported differences of up to 6 K in a deep Spanish courtyard (RA = 4.5) during summer [7,11].

Numerous studies confirm that courtyards operate as effective passive cooling strategies, particularly in hot climates. Studies show that

* Corresponding author.
E-mail addresses: alejandro.cabeza@uva.es (A. Cabeza-Prieto), mpsaez@ugr.es (M. Paz Sáez-Pérez), mcamino@uva.es (M. Soledad Camino-Olea).
[1] https://orcid.org/0000-0002-6473-2097.
[2] https://orcid.org/0000-0001-9725-1153.
[3] https://orcid.org/0000-0001-5711-3143.

https://doi.org/10.1016/j.seta.2026.104919
Received 29 July 2025; Received in revised form 20 February 2026; Accepted 4 March 2026
Available online 14 March 2026

ventilated courtyards reduce indoor temperatures in warm-humid regions [16], and that courtyard housing decreases cooling demand in Mediterranean climates [17]. Microclimates have been optimized through adaptable shading and evaporative cooling [11], with monitored thermal reductions reported in Mediterranean courtyards [18] and improvements in energy efficiency and thermal comfort observed in desert climates [19].

In recent decades, many heritage buildings have lost their original function—whether religious, residential, or institutional—leading to their rehabilitation for contemporary uses. This functional transformation is essential for their long-term conservation but introduces significant challenges in terms of thermal adaptation and energy efficiency.

In the heritage context, the rehabilitation of historic buildings after the loss of their original function has promoted the integration of courtyards into the building envelope through translucent roofs. From the nineteenth century onwards, technological advances enabled their transformation into glazed atria [20–22], substantially altering their thermal and daylight behavior compared to the original microclimate [22,23]. (Fig. 1 in the Supplementary Material).

In Europe, several studies have compared open courtyards and enclosed atria under current and future climatic conditions [22] In the Netherlands, open courtyards showed better performance under warming scenarios due to the overheating risk in enclosed atria [24]. In southwestern Germany, summer monitoring revealed higher air and radiant temperatures in glazed atria, increasing human thermal exposure [25]. In China, research on courtyard roofs concluded that these solutions can improve energy efficiency by increasing solar gains and storage, reducing heat losses, and identifying light transmittance as a key parameter [26].

Recent literature confirms that the geometry of atria and courtyards decisively conditions their thermal and energy performance. Geometric variations in atria can modify energy consumption by more than 15% [2]; In cold Chinese climates, configuration altered heating and cooling demand by 20–25% [3]. Optimization of the skylight-to-atrium ratio reduced summer operative temperature by 2–3 K while maintaining adequate daylight levels [27]. In sawtooth roofs, solar incidence angle seasonally modulates gains [28], Envelope design can reduce HVAC demand by up to 18% in extreme climates [29]. Geometry conditions insolation and shading, directly affecting seasonal comfort [30]. In massive heritage buildings, atrium energy behavior is additionally influenced by the hygrothermal response of historic masonry, whose conductivity depends non-linearly on moisture content and porosity and may differ from conventional normative values [31–33].

Despite this growing body of research, available studies mainly focus on contemporary buildings or courtyards in warm and temperate climates, whereas comparative analyses of different glazed roof geometries in historical courtyards located in cold climates remain scarce. This gap motivates the present study, which compares three translucent roof typologies applied to a Renaissance courtyard, evaluating winter and summer energy demand and thermal comfort. The study highlights the importance of rigorous design to prevent overheating and ensure year-round thermal comfort.

Materials and methods

Case study

For this study, a representative heritage building of the Renaissance palace-house typology was selected, located in the municipality of Sarracín, in the province of Burgos, Spain—an area characterized by a cold climate within the Iberian Peninsula. According to the Spanish Technical Building Code (CTE), it falls within climate zone E1 [34] and is classified as a continental Mediterranean climate (Cs) according to the Köppen–Geiger classification [35].

The building is intended for public use. The building has a total floor area of 3,794 m^2 and a window-to-wall ratio (WWR) of 12%. The courtyard has a rectangular floor plan and is surrounded by a two-story structure, with a total surface area of 310 m^2. The open courtyard measures 11.15 × 12.10 m, with a cornice height of approximately 10 m above ground level, resulting in an aspect ratio (AR = 0.82). The courtyard floor is entirely paved in stone and lacks vegetation or water surfaces, which directly influences its thermal behavior.

For this study, two simulation tools were used. Autodesk Ecotect [36] was employed to verify the climate files, calculate the solar radiation incident on each glass element, and assess the natural lighting conditions inside the space. DesignBuilder (based on EnergyPlus) [37], was used to simulate the energy demand of the new atrium space within the Renaissance palace building.

The model was simplified by defining, on the ground floor, a U-shaped conditioned space (entrance hall, chapel, and lateral rooms) and a second zone corresponding to the portico; on the first floor, the spaces were grouped into a single thermal zone around the courtyard.

Weather data

The first of the constant variables is the climate. Hourly meteorological parameters for a Typical Meteorological Year (TMY) were obtained from the U.S. Department of Energy (DOE) [37,38]. The main parameters are presented in Table S2 in the Supplementary Material.

Building model

Regarding internal gains from occupancy and equipment, internal loads were not considered, as the building is intended for occasional use (events). The modeling was conducted under free-running or demand-driven operation. Heating and cooling systems were defined using generic configurations in DesignBuilder [37,38], incorporating a

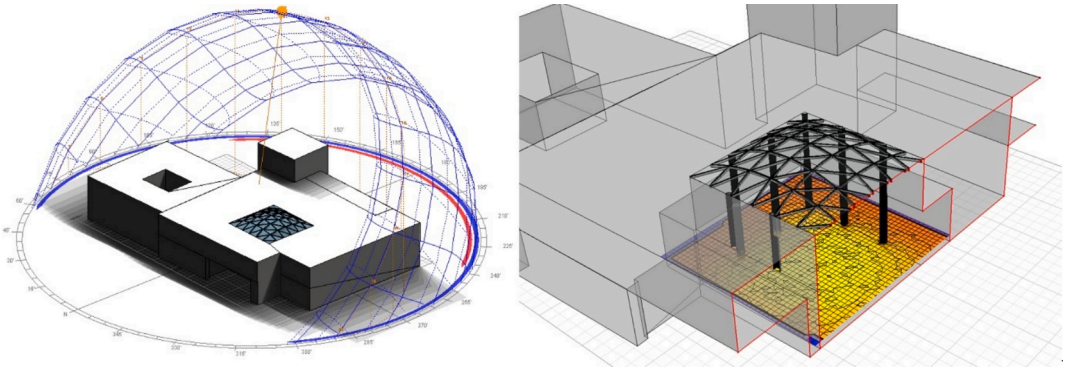

Fig. 1. Left: Building model in Autodesk Ecotect used to calculate incident solar radiation on each glass panel. Right: Example of interior lighting simulation model in Autodesk Ecotect. Grid positioned 60 cm above floor level.

simplified four-pipe fan coil HVAC system with chiller and gas boiler. A seasonal efficiency of 0.83 was assumed for the gas boiler in heating mode, while a COP of 1.67 was adopted for the cooling system, with continuous 24/7 operation and setpoints of 20 °C and 25 °C, respectively.

The envelope was defined based on on-site measurements and technical literature. Thermal and optical properties (U-value, thermal capacity, solar factor, visible transmittance, and thickness) were defined for opaque and translucent elements. These values were cross-checked against international standards (ISO 6946 [39], ISO 10456 [40], EN 673 [41] y EN 410 [42] for glazing) and manufacturers' technical data. The complete specification is provided in Table S3 of the Supplementary Material.

Roof typologies defined for the study

This study examines three architectural roof configurations designed to transform the exterior courtyard into a new interior conditioned space. The objective is to evaluate their energy performance beyond formal criteria.

- **TYPE 1.** The first solution is a triangulated semi-dome roof, frequently used in rehabilitation projects due to its adaptability. This solution consists of a semi-dome structure composed of 72 right isosceles triangles, each with leg dimensions of approximately 1.70 m and 2.60 m.
- **TYPE 2.** The second solution features a nearly flat glass roof, supported by a substructure functioning as a horizontal curtain wall with a slight slope for rainwater drainage. The structural grid includes primary beams spaced at 1.75 m intervals. The substructure consists of primary beams measuring 30 × 20 cm and secondary beams of 10 × 10 cm.
- **TYPE 3.** The third solution is a south-facing sawtooth roof, in which the vertical glass panels face south and the inclined opaque elements slope downward to the north. The vertical glass surfaces measure 1.00 m in height and 1.75 m in width. The opaque inclined panels are positioned at a 50% slope.

Simulation scenarios and assumptions

El proceso se inicia con la caracterización del edificio existente (geometría, envolvente opaca y acristalada, condiciones interiores), junto con la definición de perfiles de uso y ventilación para generar modelos energéticos representativos. Se analizaron distintos escenarios mediante simulación, estructurados en las siguientes fases.

Incident Radiation Calculation: calculated on translucent elements using a geometric model developed with Autodesk Ecotect [36].

Free-Running Simulation: The newly enclosed space was simulated under free-running conditions (with HVAC systems turned off) during representative winter and summer weeks, using DesignBuilder with the EnergyPlus 8.1 calculation engine [43]. Although free-running scenarios do not fully reproduce actual operation, they are commonly used to estimate maximum indoor temperatures and overheating degree-hours [44–46]. In this study, the free-running scenario is interpreted as a theoretical limit to compare the geometric effect of the roofs.

Annual Energy Simulation: With HVAC systems activated, an annual simulation was performed to quantify heating and cooling demand and assess the influence of roof design.

Natural Lighting Calculations: Comparative daylight calculations were carried out for the three roof types and the uncovered condition as an additional selection criterion.

To develop the three comparative models, constant variables were defined, considering the roof type as the only variable to ensure comparability of results.

To focus the analysis exclusively on the thermal performance of the roofing configurations, the model was simplified by excluding factors such as occupancy and the influence of the immediate urban surroundings (shading, reflected radiation, and wind), as their inclusion would have added complexity without directly contributing to the objective of the study.

Modeling assumptions and justification of simplifications.

To isolate the effect of roof geometry, homogeneous conditions were applied across all three typologies. A uniform ventilation and infiltration rate of 1 air change per hour (1 ACH) was considered, with continuous HVAC operation in the conditioned scenario and the exclusion of internal loads (occupancy, lighting, and equipment) both in free-running mode and in the conditioned case.

The surrounding urban context (shading and microclimatic effects) was also excluded, as the building is located in an open environment with limited shading incidence.

Although these assumptions may not fully reproduce real-use conditions, they enable a controlled comparison across typologies, ensuring that roof geometry is the only differentiating variable. Sensitivity analyses (0.5–2.0 ACH; 0–10 W/m^2) showed variations in absolute demand values but maintained the comparative hierarchy among typologies (Table S4–S5).

Incident radiation calculation

To calculate incident radiation, two complementary types of calculations were performed using Autodesk Ecotect [36] on the glazed elements of each roof in the three scenarios. First, an individual panel-by-panel analysis was carried out, geometrically determining the average daily solar radiation (Wh/m^2) incident on each panel for each calculation period (summer and winter). In this case, calculations were performed between 8:00 and 17:00 h (solar time), obtaining an average daily value for each glazed surface; these results are presented as daily averages for the winter months and the summer months.

Second, a global analysis was conducted, representing the average hourly monthly values throughout the year (i.e., hourly averages by month). The analysis considered direct and diffuse radiation based on hourly climatic data and shadow simulations derived from the building geometry, excluding shading from the urban surroundings to ensure comparability between scenarios.

Free-Running simulation

DesignBuilder software [38] was used to model the building and analyze, on an hourly basis, the thermal behavior of the atrium under the three proposed roof configurations. Energy simulations were conducted during two representative weeks. The selected summer period was from July 10 to July 17, close to the summer solstice and without climatic anomalies. For the winter simulation, the period from January 22 to January 29 was selected.

The simulations were carried out under free-running conditions, with the HVAC systems deactivated, to evaluate deviations of indoor temperatures from the thermal comfort range.

Annual energy simulation

An annual energy simulation was performed for each of the three typologies with the HVAC systems activated, in order to quantify heating and cooling demands and associated energy consumption.

The simulation provided the thermal load balance for each scenario, as well as monthly and annual heating and cooling energy demands, facilitating a controlled comparative assessment of the energy performance of each roof configuration.

Natural lighting calculations

Natural lighting was considered as a criterion for selecting the optimal roof configuration, through an analysis performed with

Autodesk Ecotect [36]. The BRE Split Flux method, based on the Daylight Factor (DF), was applied to estimate diffuse interior illuminance [47]. Fig. 1 shows the building model recreated in Autodesk Ecotect for calculating incident solar radiation on each glazing panel, together with the interior lighting simulation model.

Calculations were performed on a grid located 60 cm above the atrium floor, casting 4,096 rays per point to determine sky visibility and improve model accuracy. This approach allows the evaluation of daylight distribution under representative use conditions.

Design Sky values were derived from the horizontal illuminance exceeded 85% of the time between 9:00 and 17:00, using a value of 7564 lx calculated with the Tregenza method [48], ensuring representative unfavorable lighting conditions.

The BRE Daylight Factor method [47] also incorporates a simplified formula for internal reflections, based on total glazed area, a relative cleanliness factor (0.90 in this study), and reflectance differences between upper and lower surfaces.

Results

Incident solar radiation on glazed Roofs: Comparative evaluation of three designs

Once the geometric models of the three roof configurations were completed, annual solar radiation incident on each glazed system was analyzed. Each configuration was evaluated according to its monthly and hourly values, enabling a direct comparison of their energy performance.

Case study 01 – Triangulated Semi-Dome roof (Type 1)

In the triangulated semi-dome system (Type 1), radiation varies according to orientation. South-facing panels reach up to 1500 Wh/m^2 per day in winter, while north-facing panels do not exceed 500 Wh/m^2 per day and east- and west-facing panels are around 700 Wh/m^2 per day. In summer, radiation increases and becomes more uniformly distributed, reaching around 5000 Wh/m^2 per day, except in the least exposed north-facing panels, where values are close to 3500 Wh/m^2 per day. Due to the curvature of the dome, solar gains differ among panels.

The annual distribution (Fig. 2) shows maximum values in summer, reaching 578 Wh/m^2 at 14:00 in July, and minimum values in winter, close to 80 Wh/m^2. Due to its geometry, the dome behaves similarly to a horizontal surface, with relatively uniform and intense solar exposure, particularly in summer.

Case study 02 – Flat glazed roof (Type 2)

In the case of Type 2 (flat glazed roof), radiation is uniform across the different panels. In winter, lower values are recorded (around 1300 Wh/m^2 per day), while in summer maximum values exceed 5500 Wh/m^2 per day.

In terms of monthly values, the maximum values coincide with the highest overheating risk in summer, reaching around 640 Wh/m^2 during peak hours, while minimum values appear in January and December at approximately 87 Wh/m^2.

The annual graph (Fig. 3) shows high radiation in summer and very low values in winter, even lower than in Type 1. As in the semi-dome roof, values increase in summer and decrease in winter; however, total radiation is higher than that recorded in Type 1.

Case study 03 – Sawtooth roof (Type 3)

This configuration consists of alternating inclined opaque panels and vertical glazed panels. The glazed surfaces, all with the same orientation and geometry, receive solar radiation uniformly.

With respect to the annual graph (Fig. 4), the highest values are not recorded during the summer months, but rather in September and October, with a maximum value significantly lower than in the previous types—around 335 Wh/m^2. In June and July, values do not exceed 280 Wh/m^2. A decrease is observed between April and July, slight increases in February–March and August–November, and minimum values in December–January due to reduced solar availability.

Regarding the panel analysis, due to their parallel vertical arrangement, monthly values show less variation between seasons. Maximum values do not coincide with the highest overheating risk (see annual graph); they are recorded in September, while minimum values appear in winter, around 1360 Wh/m^2. In summer, radiation remains moderate, around 2000 Wh/m^2.

Free-Running energy simulation results

The hourly graphs allow the identification of the thermal loads that affect the indoor temperature of the new atrium in each of the three roof configurations. A gray band represents the comfort range (20–25 °C) [49].

Free-Running performance. Typical summer and winter weeks

The results of the energy simulation for the selected summer period are shown on the left side of Fig. 5. The winter week results are shown on the right side of Fig. 5.

In summer, solar gains in Type 1 and Type 2 are very high, with Type 2 exceeding 50 kWh during the central hours of the day. In contrast, Type 3 records much lower values, around 10 kWh. Heat absorption and transmission through the walls increase as glazing gains rise Fig. 6.

In Types 1 and 2, the indoor temperature remains outside the

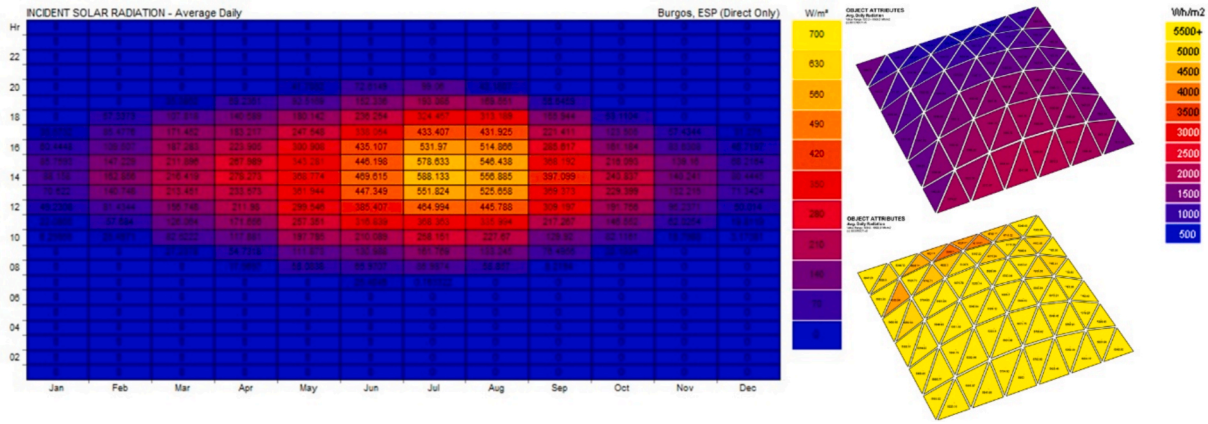

Fig. 2. TYPE 1. Average daily/hourly incident radiation (Wh/m^2). Annual calculation. On the left, incident solar radiation on glazing; above, winter months; below, summer months.

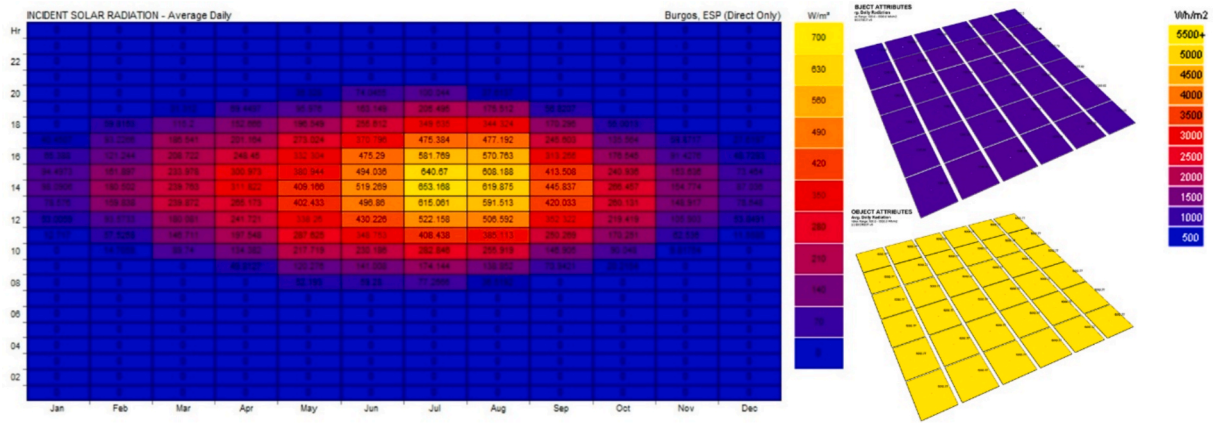

Fig. 3. TYPE 2. Average daily/hourly incident radiation (Wh/m^2). Annual calculation. On the left, incident solar radiation on glazing; above, winter months; below, summer months.

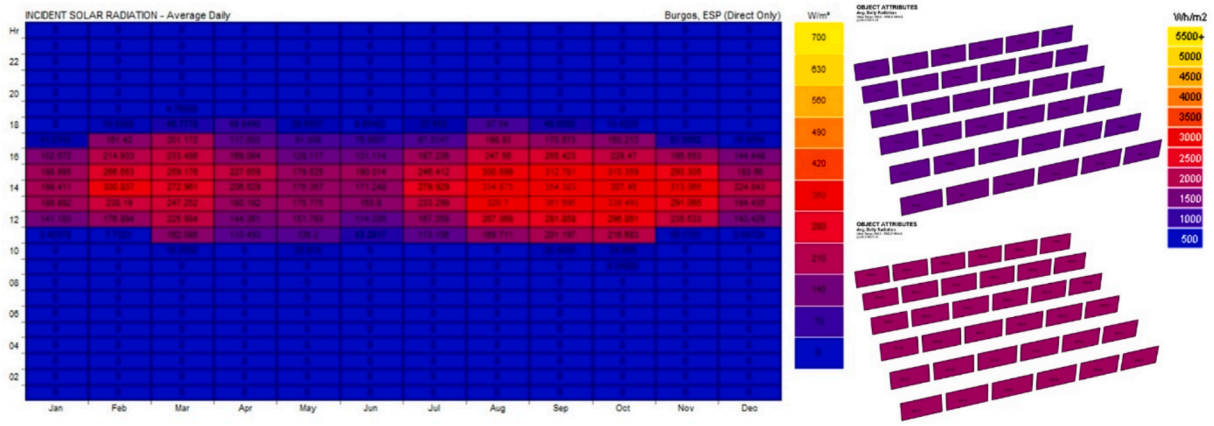

Fig. 4. TYPE 3. Average daily/hourly incident radiation (Wh/m^2). Annual calculation. On the left, incident solar radiation on glazing; above, winter months; below, summer months.

comfort range for most of the day, reaching acceptable conditions only between 00:00 and 11:00 in Type 1 and between 00:00 and 10:00 in Type 2.

In winter, solar gains reach around 19 kWh in Types 1 and 2 and exceed 25 kWh in Type 3 at certain times. However, these differences hardly affect indoor temperature under free-running conditions, which remains below the comfort range in all three cases.

Type 3 shows lower daily thermal oscillation and greater stability, while Types 1 and 2 exhibit more pronounced fluctuations. The remaining thermal loads are similar in the three scenarios.

Annual energy demand study

Monthly heating and cooling demands show clear differences between typologies. In Types 1 and 2, both services are required in certain months, with summer cooling demands exceeding 10 kWh/m^2·year, especially in July and August. In contrast, Type 3 presents virtually no cooling demand, which is particularly relevant in heritage buildings with high thermal inertia, as it favors passive control of summer temperatures [50–53]. In winter, heating behavior is similar in the three configurations, with maximum values in the coldest months.

In annual terms, Type 3 requires no cooling energy (−0.97 kWh/m^2·year), while Types 1 and 2 show similar values (26.70 and 25.80 kWh/m^2·year, respectively), representing a 3.3% reduction in Type 2. In heating demand, Type 2 presents the lowest value (197.73 kWh/m^2·year), compared to 229.26 kWh/m^2·year in Type 1 (+16%) and 211.94 kWh/m^2·year in Type 3 (+7.2% relative to Type 2).

Natural lighting results

The values were calculated on an analysis grid placed in the atrium at 60 cm above floor level. This allows the visualization of contours and *iso*-surfaces. The highest values compared to the uncovered condition are obtained in Type 1 and Type 2, reaching approximately 5400 lx. In contrast, Type 3 yields lower values, around 4200 lx, shifted toward the north due to the sawtooth roof with south-facing glazing (Fig. 7). Nevertheless, all cases largely exceed the recommended levels for this type of space (100–600 lx).

Table 1 presents the key performance indicators obtained for each roof configuration, allowing for a clear comparison of their thermal and lighting performance.

Discussion

The results clearly demonstrate the decisive influence of roof geometry on the thermal and energy performance of the new atrium. In Type 1 (semi-dome) and Type 2 (horizontal glass), the high solar incidence during warm months—reaching values above 600 Wh/m^2—led to significant thermal discomfort, consistent with [25], which warns of overheating in glazed atria. During winter months, solar gain remains reduced (around 250 Wh/m^2).

In contrast, the Type 3 solution (sawtooth roof) with south-facing vertical translucent panels exhibited a more balanced behavior. In summer, incident solar radiation did not exceed 280 Wh/m^2, while in colder months values reached 300–335 Wh/m^2, with maxima in

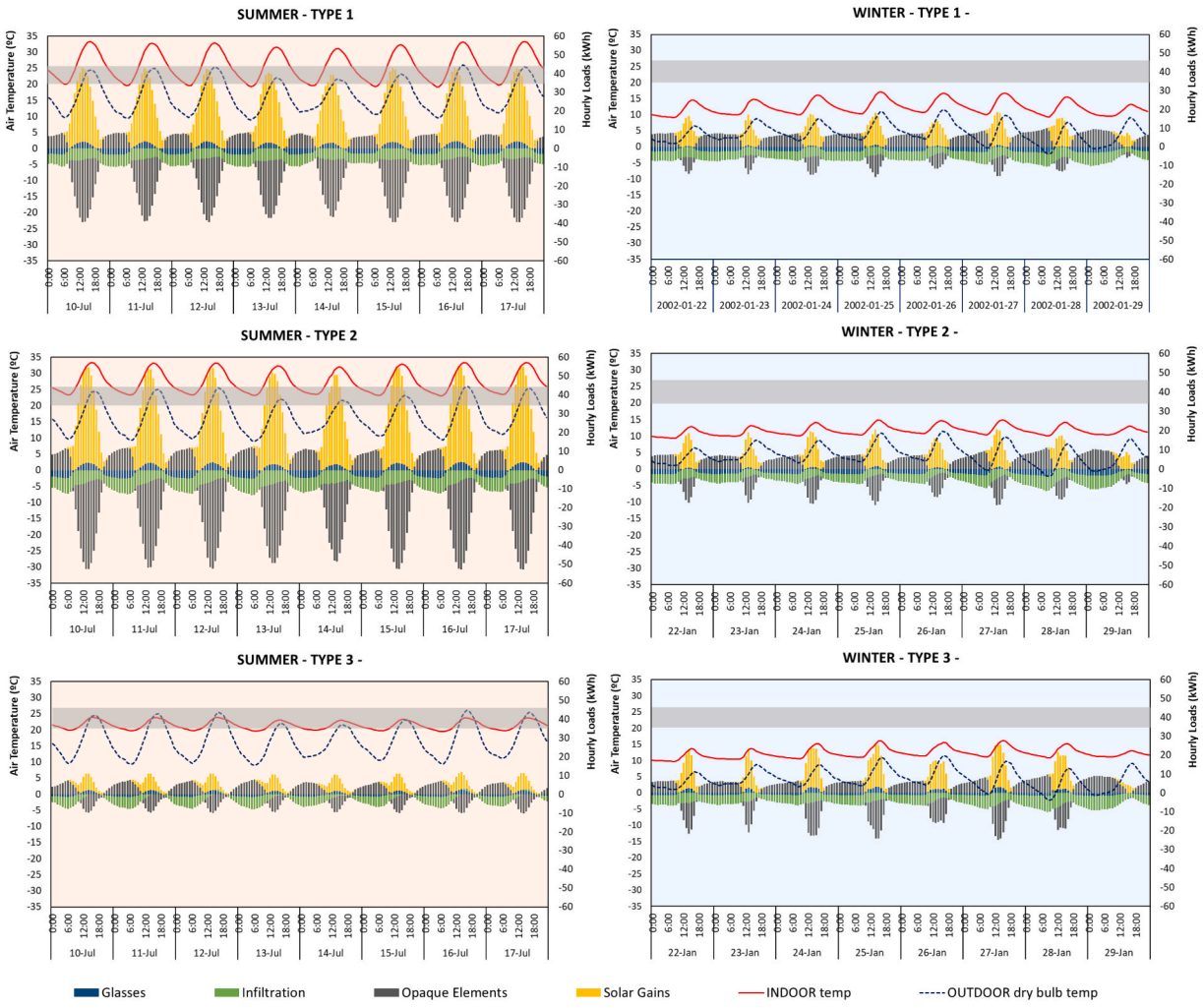

Fig. 5. Free-running simulation on an hourly basis. Winter week. Blue dashed line: outdoor dry-bulb temperature; solid red line: indoor temperature. Bars represent thermal loads. Gray band: comfort zone. (For interpretation of the references to colour in this figure legend, the reader is referred to the web version of this article.)

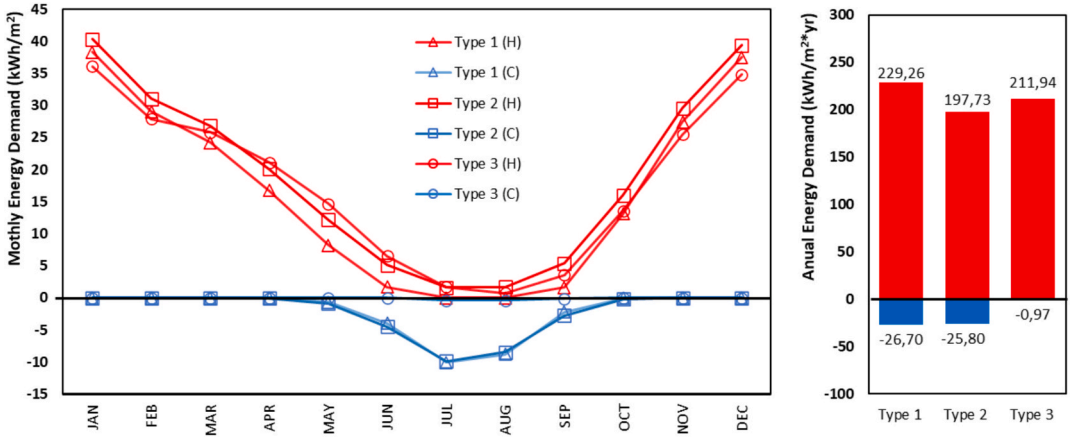

Fig. 6. Monthly and annual energy demands in kWh/m^2.

September–October (355 Wh/m^2), lower than in Types 1 and 2. This supports [26], which identifies orientation and solar transmittance as key variables for improving efficiency without inducing overheating.

Although the total incident solar radiation on translucent elements is much higher in absolute terms in Options 1 and 2, it is concentrated in summer. In Type 3, annual solar incidence is reduced during critical months and maintained in winter compared to Options 1 and 2, which is beneficial in a cold climate.

Regarding the free-running simulation, analyzing the load balance during the winter week shows no significant differences in indoor temperatures between the three roof types; in all cases, the interior temperature remains below the comfort threshold.

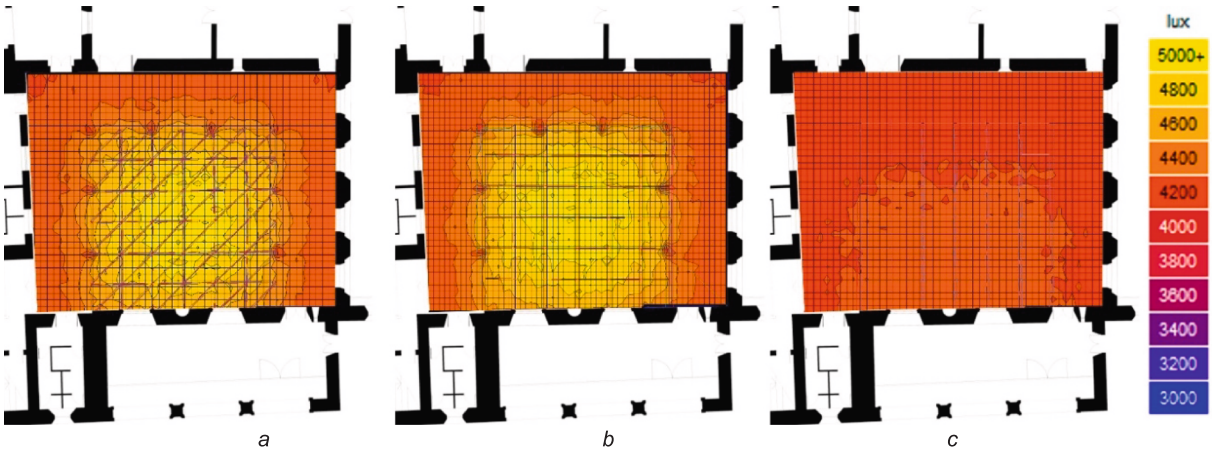

Fig. 7. Illumination levels on a grid located 60 cm above the floor plane for each of the 3 types studied from left to right: TYPE 1 (a), TYPE 2 (b), and TYPE 3 (c).

Table 1
Summarizes the key performance indicators obtained for each roof configuration, facilitating a comparative understanding of their thermal and lighting behavior.

Variable	Type 1: Semi-Dome	Type 2: Flat Roof	Type 3: Sawtooth Roof
Cooling demand (kWh/m^2·year)	26.7	25.8	0.0
Heating demand (kWh/m^2·year)	229.3	197.7	211.9
Max. indoor temp (summer, °C)	35.0	35.0	24.0
Thermal swing (summer, °C)	15	22	4
Avg. illuminance (lux)	~5400	~5400	~4200
Comfort hours (free-running, summer)	<40%	<30%	>95%
Solar gain in winter (Wh/m^2)	~250	~200	~335
Solar gain in summer (Wh/m^2)	>500	>600	<280

In summer, Types 1 and 2 exceeded the comfort range, with temperatures above 33 °C, while Type 3 remained between 20 and 24 °C. The daily thermal oscillation reached 15 °C in Type 1, 22 °C in Type 2, and only 4 °C in Type 3, whose stability is supported by the high thermal inertia of the building, consistent with [50,51]. This behavior is also influenced by the hygrothermal response of massive historic masonry, whose thermal conductivity varies with moisture content and porosity, as demonstrated by recent experimental studies [31–33].

The annual energy demand analysis reinforces these conclusions. The Type 3 system exhibits virtually no cooling demand, compared to values close to 26 kWh/m^2·year in Types 1 and 2, in line with [52] and with studies relating geometry and thermal behaviour [12].

Although [24,25] associate enclosed atria with increased thermal exposure, this study demonstrates that an appropriate bioclimatic design, based on solar control and south-facing vertical orientation, can minimize summer gains without losing winter solar capture, as noted by [26,54].

Several studies have quantified the impact of geometry on the energy performance of atria and courtyards. [28] reported reductions greater than 15% in total energy consumption depending on atrium shape. [29] observed differences of 20–25% in heating and cooling demand for an enclosed atrium in a cold Chinese climate as a function of its geometric configuration. [27] demonstrated that optimizing the skylight-to-atrium ratio could decrease operative summer temperature by approximately 2–3 K while maintaining adequate daylight conditions. In hot-summer cold-winter regions, [32] reported reductions of up to 18% in energy demand through optimized courtyard envelope design. [28] confirmed that the inclination and orientation of sawtooth roofs seasonally alter solar gains. These data support the superiority of Type 3 and nuance the conclusions [24,25].

The discrepancy with previous studies is explained by the south-facing vertical glazing of the sawtooth roof. In summer, high solar altitude reduces incidence on vertical surfaces; in winter, more perpendicular incidence enhances solar capture, consistent with [28]. The near-zero cooling demand is also related to the assumption of no internal gains; when included cooling loads remain lower according to the sensitivity analysis.

Beyond geometry, thermal mass and thermal bridges influence performance. In the model, inertia was considered (Table S3), contributing to the observed stability; the literature indicates that higher solar transmittance increases winter gains but also summer risk, while greater inertia improves stability [50,55].

Regarding natural lighting, although Type 3 provides lower illuminance levels than the other systems, it still exceeds 4000 lx, demonstrating that solar control and adequate daylight can coexist without compromising thermal comfort.

Study Limitations

As noted by [56], modeling adaptive envelopes requires balancing contextual precision and computational feasibility, justifying the use of controlled comparative models.

This exploratory study isolated the geometric effect of roof typologies through explicit methodological simplifications.

The influence of the immediate urban context, including shadows, wind, or urban ventilation, was not considered in order to ensure a reproducible environment. In the selected Renaissance palace, surrounded by open space, shading effects are expected to be minor, especially in summer. However, in denser urban contexts such factors should be evaluated in future research.

No realistic usage profiles or internal loads were modeled. Thermal demands therefore correspond to a baseline scenario without internal gains. HVAC systems were assumed to be continuously available (24/7) with constant setpoint temperatures of 20 °C for heating and 25 °C for cooling. Active natural ventilation was not modeled; instead, a uniform infiltration rate of 1 air change per hour was applied. These assumptions allow systematic comparison, although they limit direct extrapolation to real conditions.

Thermal bridges were not modeled; however, since they were excluded from all typologies, the relative comparison remains valid.

To address uncertainty, sensitivity analyses were conducted. Heating demand varied by –40% to + 95% depending on infiltration rates (0.5–2.0 ACH) and decreased by up to 30% with higher internal gains (0–10 W/m^2). Cooling demand increased by 10% to 80% under higher internal gains, although on low absolute values in this cold climate. While absolute demands change, the comparative hierarchy among typologies remains unchanged.

No monitoring data are available; validation was therefore addressed indirectly through comparison with the literature, verification of physical consistency, and plausibility in similar climates. This limitation is acknowledged, and future validation through monitoring campaigns in comparable heritage courtyards is proposed.

Practical Implications.

The findings of this study offer design criteria for the energy rehabilitation of historic courtyards in cold climates with progressively warmer summers.

- The sawtooth roof configuration, featuring south-oriented vertical glazing, maintains thermal comfort in summer under passive conditions and eliminates the need for active cooling systems. This solution balances winter solar capture and summer control.
- Flat and dome-shaped glazed roofs pose greater thermal risk if not complemented by shading devices or selective glazing.
- Roof geometry directly affects thermal stability and energy demand. In the case analyzed, selecting the appropriate geometric configuration reduced cooling energy demand by 100% without compromising daylight availability or winter comfort.
- The comparative methodology used in this study is replicable in other heritage contexts and supports decision-making that integrates conservation and climate adaptation.
- Passive geometric solutions reduce dependence on mechanical systems, favouring architectural preservation.

Architectural Compatibility and Heritage Constraints.

Although the south-facing sawtooth roof with vertical glazing showed the best performance, its contemporary language may generate tensions with conservation criteria. However, it can be compatible with heritage values through lightweight structures, slim profiles, or reversible solutions, allowing efficiency and conservation to coexist. This configuration constitutes a technically valid alternative, particularly in reversible interventions. The study does not propose a universal solution, but rather a quantitative basis for balancing conservation and environmental performance.

Climate Resilience and Future Relevance of the Study.

Although future climate scenarios were not explicitly modeled, the results allow anticipation of the relative behaviour of each typology under warmer summers and increased overheating risk. In this context, the sawtooth configuration emerges as a climate-resilient passive solution: it limits summer gains while maintaining winter capture, ensuring comfort without active cooling.

While projected datasets (e.g., RCP 4.5 or 8.5) were not used, the comparative framework developed provides a solid basis for evaluating roof geometries under future climate contexts.

Conclusions

This study has evaluated the impact of three translucent roof typologies applied to a historical courtyard, analyzing their thermal behavior, energy demand, and natural lighting performance. The results confirm that the geometry and orientation of the roof have a decisive influence on the environmental performance of the atrium. These variables directly influence comfort and energy efficiency, particularly under increasing cooling demand scenarios.

The sawtooth roof with south-facing vertical glazing (Type 3) showed the best seasonal balance. Despite having a smaller glazed surface, it maximized winter solar capture (up to 335 Wh/m^2) and limited summer incidence (less than 275 Wh/m^2), thus avoiding overheating. Under free-running conditions, it maintained indoor temperatures within the comfort range throughout the summer week, with no cooling demand. In contrast, Type 1 and Type 2 solutions produced high thermal loads in summer, with cooling demands near 26 kWh/m^2·year, compromising both thermal comfort and energy efficiency.

These results qualify previous studies associating enclosed atria with generalized overheating, demonstrating that a bioclimatic design based on orientation, glazing proportion, and solar control allows winter optimization and summer mitigation. Therefore, the selection of geometry, orientation, and glazing ratio must be a central design criterion in interventions involving historical courtyards.

The methodology used is transferable to similar contexts and provides a technical basis for sustainable heritage rehabilitation integrating conservation, comfort, and energy efficiency.

The robustness of these conclusions was confirmed by sensitivity analyses on infiltration and internal loads, which preserved the comparative hierarchy among roof types. Nevertheless, future validation through monitoring campaigns in comparable heritage courtyards, as well as simulations including realistic occupancy profiles and climate change scenarios, is recommended to refine the absolute values and further consolidate these findings.

Declaration of Generative AI and AI-assisted technologies in the writing process

During the preparation of this work the authors used ChatGPT (OpenAI) in order to improve language and readability. After using this tool/service, the authors reviewed and edited the content as needed and takes full responsibility for the content of the publication.

CRediT authorship contribution statement

Alejandro Cabeza-Prieto: Writing – review & editing, Writing – original draft, Visualization, Validation, Supervision, Methodology, Investigation, Formal analysis, Data curation, Conceptualization. **M. Paz Sáez-Pérez:** Writing – review & editing, Writing – original draft, Visualization, Validation, Supervision, Methodology, Investigation, Formal analysis, Data curation, Conceptualization. **M. Soledad Camino-Olea:** Validation, Supervision, Investigation, Funding acquisition.

Declaration of competing interest

The authors declare that they have no known competing financial interests or personal relationships that could have appeared to influence the work reported in this paper.

Acknowledgements

The authors would like to thank the reviewers for their thoughtful comments and efforts towards improving our manuscript. This article is part of the research activities of the project "PID-2022 Project, 139363NB-I00, titled *Evaluation of the improvement in energy efficiency of thick exposed brick façades through active air cavities (EvELaC)*," funded by MICIU/AEI /10.13039/501100011033 and by FEDER, EU as well as by the project *"Propuesta de rehabilitación energética de plantas bajo la cubierta, calientes en verano y frías en invierno: biblioteca ETSA y edificio Soria,"* funded by Universidad de Valladolid (2024 call for projects on energy efficiency and renewable energy in university buildings).

Appendix A. Supplementary data

Supplementary data to this article can be found online at https://doi.org/10.1016/j.seta.2026.104919.

Data availability

Data will be made available on request.

References

[1] Aldawoud A. Thermal performance of courtyard buildings. Energ Buildings 2008; 40:906–10. https://doi.org/10.1016/J.ENBUILD.2007.07.007.

[2] Aldawoud A. The influence of the atrium geometry on the building energy performance. Energ Buildings 2013;57:1–5. https://doi.org/10.1016/j.enbuild.2012.10.038.

[3] Wang L, Huang Q, Zhang Q, Xu H, Yuen RKK. Role of atrium geometry in building energy consumption: the case of a fully air-conditioned enclosed atrium in cold climates, China. Energ Buildings 2017;151:228–41. https://doi.org/10.1016/j.enbuild.2017.06.064.

[4] Ghaffarianhoseini A, Berardi U, Ghaffarianhoseini A. Thermal performance characteristics of unshaded courtyards in hot and humid climates. Build Environ 2015;87:154–68. https://doi.org/10.1016/J.BUILDENV.2015.02.001.

[5] Martinelli L, Matzarakis A. Influence of height/width proportions on the thermal comfort of courtyard typology for Italian climate zones. Sustain Cities Soc 2017;29: 97–106. https://doi.org/10.1016/J.SCS.2016.12.004.

[6] Zhu J, Feng J, Lu J, Chen Y, Li W, Lian P, et al. A Review of the Influence of Courtyard Geometry and Orientation on Microclimate. Build Environ 2023;236: 110269. https://doi.org/10.1016/j.buildenv.2023.110269.

[7] Lopez-Cabeza VP, Alzate-Gaviria S, Diz-Mellado E, Rivera-Gomez C, Galan-Marin C. Albedo influence on the microclimate and thermal comfort of courtyards under Mediterranean hot summer climate conditions. Sustain Cities Soc 2022;81: 103872. https://doi.org/10.1016/J.SCS.2022.103872.

[8] Rodríguez-Algeciras J, Tablada A, Chaos-Yeras M, De la Paz G, Matzarakis A. Influence of aspect ratio and orientation on large courtyard thermal conditions in the historical centre of Camagüey-Cuba. Renew Energy 2018;125:840–56. https://doi.org/10.1016/J.RENENE.2018.01.082.

[9] Almhafdy A, Ibrahim N, Ahmad SS, Yahya J. Courtyard Design Variants and Microclimate Performance. Procedia Soc Behav Sci 2013;101:170–80. https://doi.org/10.1016/j.sbspro.2013.07.190.

[10] Salameh M, Taleb H. Courtyard as passive design solution for school buildings in hot area. World Congress on Civil, Structural, and Environmental Engineering, Avestia Publishing 2017. https://doi.org/10.11159/awspt17.141.

[11] Diz-Mellado E, López-Cabeza VP, Rivera-Gómez C, Naboni E, Galán-Marín C. Optimizing a courtyard microclimate with adaptable shading and evaporative cooling in a hot mediterranean climate. Journal of Building Engineering 2024;88: 109167. https://doi.org/10.1016/J.JOBE.2024.109167.

[12] Salameh M, Touqan B. Designing Climate-Adaptive buildings: Impact of Courtyard Geometry on Microclimates in Hot, Dry Environments. Civil Engineering Journal (Iran) 2024;10:2698–718. https://doi.org/10.28991/CEJ-2024-010-08-017.

[13] Bulus M, Hamid M, Lim YW. Courtyard as a Passive Cooling Strategy in buildings. International Journal of Built Environment and Sustainability 2017;4.

[14] Forouzandeh A. Numerical modeling validation for the microclimate thermal condition of semi-closed courtyard spaces between buildings. Sustain Cities Soc 2018;36:327–45. https://doi.org/10.1016/j.scs.2017.07.025.

[15] Rajapaksha I, Nagai H, Okumiya M. A ventilated courtyard as a passive cooling strategy in the warm humid tropics. Renew Energy 2003;28:1755–78. https://doi.org/10.1016/S0960-1481(03)00012-0.

[16] Soflaei F, Shokouhian M, Tabadkani A, Moslehi H, Berardi U. A simulation-based model for courtyard housing design based on adaptive thermal comfort. Journal of Building Engineering 2020:31. https://doi.org/10.1016/j.jobe.2020.101335.

[17] Sánchez de la Flor FJ, Ruiz-Pardo Á, Diz-Mellado E, Rivera-Gómez C, Galán-Marín C. Assessing the impact of courtyards in cooling energy demand in buildings. J Clean Prod 2021:320. https://doi.org/10.1016/j.jclepro.2021.128742.

[18] Jara E ángel R, de la Flor FJS, Domínguez SÁ, Lissén JMS, Casado AR. Characterizing the air temperature drop in Mediterranean courtyards from monitoring campaigns. Sustainability (Switzerland) 2017;9. doi:10.3390/su9081401.

[19] Zamani Z, Heidari S, Azmoodeh M, Taleghani M. Energy performance and summer thermal comfort of traditional courtyard buildings in a desert climate. Environ. Prog. Sustain Energy 2019:38. https://doi.org/10.1002/ep.13256.

[20] Sharples S, Bensalem R. Airflow in courtyard and atrium buildings in the urban environment: a win tunnel study. Sol Energy 2001;70:237–44. https://doi.org/10.1016/S0038-092X(00)00092-X.

[21] Moosavi L, Mahyuddin N, Ab Ghafar N, Azzam IM. Thermal performance of atria: an overview of natural ventilation effective designs. Renew Sustain Energy Rev 2014;34:654–70. https://doi.org/10.1016/j.rser.2014.02.035.

[22] Aldawoud A, Clark R. Comparative analysis of energy performance between courtyard and atrium in buildings. Energ Buildings 2008;40:209–14. https://doi.org/10.1016/j.enbuild.2007.02.017.

[23] Li DHW, Cheung ACK, Chow SKH, Lee EWM. Study of daylight data and lighting energy savings for atrium corridors with lighting dimming controls. Energ Buildings 2014;72:457–64. https://doi.org/10.1016/J.ENBUILD.2013.12.027.

[24] Taleghani M, Tenpierik M, van den Dobbelsteen A. Energy performance and thermal comfort of courtyard/atrium dwellings in the Netherlands in the light of climate change. Renew Energy 2014;63:486–97. https://doi.org/10.1016/j.renene.2013.09.028.

[25] Lee H, Oertel A, Mayer H. Enhanced human heat exposure in summer in a central European courtyard subsequently roofed with transparent ETFE foil cushions. Urban Clim 2022:44. https://doi.org/10.1016/j.uclim.2022.101210.

[26] Wen B, Yang Q, Xu F, Zhou J, Zhang R. Phenomenon of courtyards being roofed and its significance for building energy efficiency. Energ Buildings 2023:295. https://doi.org/10.1016/j.enbuild.2023.113282.

[27] Wu P, Zhou J, Li N. Influences of atrium geometry on the lighting and thermal environments in summer: CFD simulation based on-site measurements for validation. Build Environ 2021;197. https://doi.org/10.1016/j.buildenv.2021.107853.

[28] de Luis FJ, Pérez-García M. Parametric study of solar gains in saw-tooth roofs facing the equator. Renew Energy 2004;29:1223–41. https://doi.org/10.1016/j.renene.2003.12.010.

[29] He C, Tian W, Shao Z. Impacts of Courtyard Envelope Design on Energy Performance in the Hot Summer–Cold Winter Region of China. Buildings 2022;12.

[30] Muhaisen AS. Shading simulation of the courtyard form in different climatic regions. Build Environ 2006;41:1731–41. https://doi.org/10.1016/j.buildenv.2005.07.016.

[31] Cabeza-Prieto A, Camino-Olea MS, Rodríguez-Esteban MA, Llorente-Álvarez A, Pérez MPS. Moisture influence on the thermal operation of the late 19th century brick facade, in a historic building in the city of zamora. Energies (Basel) 2020;13.

[32] Llorente-Alvarez A, Camino-Olea MS, Cabeza-Prieto A, Saez-Perez MP, Rodríguez-Esteban MA. The thermal conductivity of the masonry of handmade brick Cultural Heritage with respect to density and humidity. J Cult Herit 2022;53:212–9. https://doi.org/10.1016/j.culher.2021.12.004.

[33] Cabeza-Prieto A, Camino-Olea MS, Sáez-Pérez MP, Llorente-álvarez A, Gavilán ABR, Rodríguez-Esteban MA. Comparative Analysis of the thermal Conductivity of Handmade and Mechanical Bricks used in the Cultural Heritage. Materials 2022;15.

[34] Ministerio de Vivienda. Real Decreto 314/2006, de 17 de marzo, por el que se aprueba el Código Técnico de la Edificación, (2006) 11816–11831. 2006.

[35] Beck HE, Zimmermann NE, McVicar TR, Vergopolan N, Berg A, Wood EF. Present and future köppen-geiger climate classification maps at 1-km resolution. Sci Data 2018:5. https://doi.org/10.1038/sdata.2018.214.

[36] Autodesk Ecotect Analysis 2011 2011.

[37] EnergyPlus n.d. https://energyplus.net/weather-region/europe_wmo_region_6/ESP (accessed March 6, 2022).

[38] Design Builder 7.0.2.006 n.d.

[39] AENOR. UNE-EN_ISO_6946=2021(EN). AENOR; 2021.

[40] AENOR. UNE-EN ISO 10456. 2013.

[41] AENOR. UNE-EN 673. 2025.

[42] AENOR. UNE-EN 410:2011 VIDRIO PARA EDIFICACION. Determinación de las características luminosas y solares de los acristalamientos. 2011.

[43] US Department of Energy. Energy plus 2014.

[44] Inard C, Pfafferott J, Ghiaus C. Free-running temperature and potential for free cooling by ventilation: a case study. Energ Buildings 2011;43:2705–11. https://doi.org/10.1016/j.enbuild.2011.06.017.

[45] Ghiaus C. Free-running building temperature and HVAC climatic suitability. n.d.

[46] Rahif R, Amaripadath D, Attia S. Review on Time-Integrated Overheating Evaluation Methods for Residential buildings in Temperate Climates of Europe. Energ Buildings 2021:252. https://doi.org/10.1016/j.enbuild.2021.111463.

[47] Littlefair PJ. Site layout planning for daylight and sunlight: A guide to good practice. bre press; 2011.

[48] Wittkopf SK, Soon LK. Analysing sky luminance scans and predicting frequent sky patterns in Singapore. Light Res Technol 2007;39:31–51. https://doi.org/10.1177/1365782806070683.

[49] Relgamento de Instalaciones Térmicas de los Edificios. España: Boletín Oficial del Estado, 207, 1–xx; 2007.

[50] Aste N, Angelotti A, Buzzetti M. The influence of the external walls thermal inertia on the energy performance of well insulated buildings. Energ Buildings 2009;41: 1181–7. https://doi.org/10.1016/j.enbuild.2009.06.005.

[51] Orosa JA, Oliveira AC. A field study on building inertia and its effects on indoor thermal environment. Renew Energy 2012;37:89–96. https://doi.org/10.1016/j.renene.2011.06.009.

[52] Canas I, Martín S. Recovery of Spanish vernacular construction as a model of bioclimatic architecture. Build Environ 2004;39:1477–95. https://doi.org/10.1016/j.buildenv.2004.04.007.

[53] Stéphan E, Cantin R, Caucheteux A, Tasca-Guernouti S, Michel P. Experimental assessment of thermal inertia in insulated and non-insulated old limestone buildings. Build Environ 2014;80:241–8. https://doi.org/10.1016/j.buildenv.2014.05.035.

[54] Al-Dawoud A-S. ORIGINAL ARCHIVAL COPY COMPARATIVE ANALYSIS OF ENERGY PERFORMANCE BETWEEN COURTYARD AND ATRIUM IN BUILDINGS. 2006.

[55] Cabeza-Prieto A, Sánchez-Guevara Sánchez C, Camino Olea MS. ESTUDIO DE LA CONTRIBUCIÓN DE LA INERCIA TÉRMICA AL COMPORTAMIENTO TÉRMICO DE EDIFICIOS. n.d.

[56] Loonen RCGM, Favoino F, Hensen JLM, Overend M. Review of current status, requirements and opportunities for building performance simulation of adaptive facades. J Build Perform Simul 2017;10:205–23. https://doi.org/10.1080/19401493.2016.1152303.